

Estimation of centrality and time dependence of anisotropic transverse flow in Au+Au collisions

A. M. Adare, J. L. Nagle, P.W. Stankus¹

¹*PHENIX Institutions*

(Dated: October 15, 2004)

Abstract

We use the Monte Carlo method to study the influence of free-streaming time and centrality on the azimuthal distribution of secondary particles produced in ultrarelativistic $Au+Au$ collisions. We compare three different distributions of nuclear collision participants in our model, and demonstrate that the eccentricity of the transverse flow pattern decreases with free-streaming time, and that this reduction in eccentricity occurs more quickly in peripheral collisions. The time dependence of the eccentricity is found to agree closely with an analytic free-streaming model, thus serving as a confirmation of the quantitative time-evolution of the eccentricity in the free-streaming approximation. The effect of the diffuse outer region of the Woods-Saxon nuclear density profile on the eccentricity is also studied, and it is found that the contribution from collisions involving this part of the distribution is significant, especially in more peripheral events.

PACS numbers:

In ultrarelativistic heavy-ion collisions, the overlapping impact region can be approximated as an elliptically-shaped distribution of secondary particles whose eccentricity depends on impact centrality and the intrinsic deformation of the colliding nuclei. If both nuclei are centered on the x -axis, the spatial eccentricity is defined as

$$\epsilon(x, y, \Delta t) = \frac{\langle y^2 \rangle - \langle x^2 \rangle}{\langle y^2 \rangle + \langle x^2 \rangle}, \quad (1)$$

where the angle brackets denote RMS averages over the x - y distribution of participant nucleons at a fixed time. The participant distribution can be used as an estimate of the initial energy density in the transverse plane. The eccentricity is of interest in the study of thermalization of the matter formed at RHIC because of its relation to the elliptic flow coefficient v_2 , which describes the azimuthal distribution of particles with respect to the reaction plane:

$$\frac{d^2 N}{d\phi dP_T} = \frac{dN}{dP_T} (1 + 2v_2(p_T) \cos(2\phi)). \quad (2)$$

PHENIX measurements have indicated that at low p_T , the ratio v_2/ϵ is roughly independent of centrality over the mid-central region (Fig. 1), which supports predictions from transport theory and hydrodynamics models [1–3]. It can therefore be assumed that ϵ scales with v_2 such that the observation of a fractional reduction in eccentricity is tantamount to observing a fractional reduction in v_2 .

In this analysis we investigate $Au+Au$ collisions at impact parameters of ranging from 2 to 12 fm. We take the nuclear radius to be isotropically uniform, neglecting any intrinsic nuclear deformation. We take the cross-section σ_{NN} to be 42 mb at full RHIC beam energy. The space-time evolution of the secondary particle distribution is influenced by the initial energy density of collision participants [4] as well as hydrodynamic pressure gradients [1]. We allow the particles to flow freely in random directions with the assumption that thermalization occurs abruptly afterwards, and we do not take hydrodynamics, phase transitions, or scattering processes into account.

Our model employs a Monte Carlo algorithm in which the regions occupied by the colliding nuclei are filled with random points placed according to a specified distribution of collision participants. A simple flat circular distribution (constant $d^2 N_{part}/dx dy$) and collision participant density functions calculated from hard-sphere and Woods-Saxon profiles are compared. The nuclear thickness functions $T_A(x, y)$ and $T_B(x - b, y)$ used in the participant

distribution are the projections of spherical nuclei A or B onto the transverse plane:

$$T_{A,B}(x, y) = \int dz \rho_{A,B}(x, y, z). \quad (3)$$

We obtain the normalization factor by requiring the thickness function to return the original number of nucleons when integrated over the transverse plane: $N \int dxdy T_{A,B}(x, y) = A$. In the hard-sphere approximation we assume $\rho(x, y, z)$ is constant, and we obtain for nucleus A centered at $(x, y) = (0, 0)$ and nucleus B centered at $(x, y) = (b, 0)$

$$T_A(x, y) = \frac{3A}{2\pi R^3} \sqrt{R^2 - x^2 - y^2}, \quad T_B(x - b, y) = \frac{3A}{2\pi R^3} \sqrt{R^2 - (x - b)^2 - y^2}. \quad (4)$$

It is assumed that the thickness drops to zero as a step function outside the nuclear radii.

The nuclear thickness function for the Woods-Saxon profile is found by numerically integrating the nuclear density

$$\rho(r) = \frac{\rho_0}{1 + \exp[\frac{r-R}{a}]} \quad (5)$$

over the transverse plane, where the parameters $R = 6.38$ fm and $a = 0.54$ fm are used for the Au nucleus [9].

Whatever the nuclear density profile used, the probabilities for interaction must be taken into account to compute the collision participant distribution. For an interaction between a single nucleon and nucleus A , the mean number of interactions is $\langle N_{int} \rangle = \sigma_{NN} T_A(x, y)$, and if the number of interactions suffered by the nucleon is assumed to follow a Poisson distribution, the probability to interact is $1 - \text{Prob}(\langle N_{int} \rangle = 0)$, or $1 - \exp(-\langle N_{int} \rangle)$. If the single nucleon is then replaced by nucleus B , the contribution to the participant density from nucleus B is

$$\frac{d^2 N_B}{dxdy} = T_B(x - b, y) (1 - \exp[-\sigma_{NN} T_A(x, y)]). \quad (6)$$

The contribution from nucleus A will have a similar form, and the total participant density function is the sum of the two contributions:

$$\frac{d^2 N_{part}}{dxdy} = T_A(x, y) (1 - \exp[-\sigma_{NN} T_B(x - b, y)]) + T_B(x - b, y) (1 - \exp[-\sigma_{NN} T_A(x, y)]). \quad (7)$$

For all of the density models tested, the secondary particles occupying the overlap region are given a velocity of c in random azimuthal directions, and are then allowed to travel for 4 fm/ c . The positions are recorded at each interval of 0.5 fm/ c . Although an oversimplification, this

approach provides a reasonable starting point for obtaining a first-order estimate of the elliptic flow evolution.

As a check, the results are compared with an analytic model proposed by Kolb *et al* [1] which employs similar assumptions (*i.e.* free-streaming before immediate thermalization) but uses a Gaussian particle distribution in phase space for the initial ellipse:

$$f(\mathbf{r}, \mathbf{p}, t_0) = \exp \left[-\frac{x^2}{2R_x^2} - \frac{y^2}{2R_y^2} - \frac{p_x^2 + p_y^2}{2\Delta^2} \right]. \quad (8)$$

With this parametrization the time dependence of the elliptic flow can be written as

$$\frac{\epsilon(t_0 + \Delta t)}{\epsilon(t_0)} = \left[1 + \frac{(c\Delta t)^2}{\langle r^2 \rangle} \right]^{-1}. \quad (9)$$

The parameters R_x and R_y in eq. (8) are the width and height of the initial ellipse, and the quantity $\langle r^2 \rangle$ in eq. (9) is the angle-averaged squared radius of the ellipse formed by N secondary particles:

$$\langle r^2 \rangle = \sum_{i=1}^N \frac{x_i^2 + y_i^2}{N} \quad (10)$$

Equation (9) is plotted together in fig. (2) with the result of the Monte Carlo calculations using the $\langle r^2 \rangle$ values computed for each timestep and impact parameter. The agreement between the Monte Carlo results and eq. (9) is quite close for the three different models, and the curves for the models are similar to each other, suggesting that the time evolution of the eccentricity in the free-streaming approximation does not depend sensitively on the nuclear density profile.

The initial eccentricities for the hard-sphere and Woods-Saxon distributions are plotted in fig. (3) with results from a Glauber Monte-Carlo calculation by K. Reyers [10]. The eccentricities for the hard-sphere distribution are higher than those of the Glauber model by a factor of 2, while The Woods-Saxon eccentricities agree within a few percent up in the central and mid-central region. Because the Glauber model by Reyers employs a Woods-Saxon distribution with the same parameters, this is expected, but it suggests that initial eccentricity of the elliptic region is highly model-dependent, despite the fact that the time evolution of the elliptic dilution is not. The contribution to the elliptic distribution of the outermost particles in the Woods-Saxon profile is examined by restricting the size of the distribution at various cutoff radii. If the full Woods-Saxon profile is truncated at a cutoff radius $r_c = 10.3$ fm, the initial eccentricities agree very closely with the Glauber values. The

initial eccentricities are sensitively dependent on the r_c value chosen, and range from the lowest curve in fig. (3) ($r_c = \infty$) to the hard-sphere curve as r_c approaches the hard-sphere radius. The contribution to the initial eccentricity of the particles lying within and outside the R parameter of eq. () is shown as a function of impact parameter in fig (4). If we denote the particles residing at $r < R$ and $r > R$ as $r_<$ and $r_>$, it can be seen that $r_< + r_<$ collisions make a small contribution to the ellipse, while $r_< + r_>$ collisions are significant at all centralities, and in fact become the dominant contribution to the number of particles in the ellipse in the most peripheral events. This serves to further illustrate that the diffuse region in the “tail” of the Woods-Saxon profile is a large contributor to the particle distribution composing the ellipse, and should not be neglected in the construction of theoretical models.

To summarize, we observe a reduction in eccentricity with time for the three nuclear density distributions in tested in our model, and a sharper reduction in eccentricity with time at larger impact parameters. This behavior is quantitatively consistent with the analytic free-streaming model of Kolb *et al* that is based on a Gaussian particle distribution, and suggests that the nuclear density profile is not of primary importance in determining the time evolution of the elliptic flow in the free-streaming approximation. The initial eccentricities, however, depend upon the nuclear thickness function used, and the full Woods-Saxon profile should be accounted for in transport and hydrodynamics models of heavy-ion collisions.

We thank the staff of the Collider-Accelerator and Physics Departments at BNL for their vital contributions. We acknowledge support from the Department of Energy and NSF (U.S.A.), MEXT and JSPS (Japan), RAS, RMAE, and RMS (Russia), BMBF, DAAD, and AvH (Germany), VR and KAW (Sweden), CNPq and FAPESP (Brazil), IN2P3/CNRS and ARMINES (France), OTKA (Hungary), DAE and DST (India), KRF and CHEP (Korea), U.S. CRDF for the FSU, US-Hungarian NSF-OTKA-MTA, and US-Israel BSF.

-
- [1] P.F. Kolb, J. Sollfrank, U. Heinz, hep-ph/0006129 v2 (2003).
 - [2] J.Y. Ollitrault, Phys. Rev. **D46** 229 (1992).
 - [3] H. Sorge, Phys. Rev. Lett. **82** 2048 (1999)
 - [4] C.Y. Wong, Phys. Rev. **D30** 961 (1984).
 - [5] C.Y. Wong, “Introduction to High-Energy Heavy Ion Collisions”, p.262, World Scientific Pub-

- lishing Co. Pte. Ltd.(1994).
- [6] K. Adcox *et al.*, Phys Rev. Lett. **89** 212301 (2002)
 - [7] K. Adcox *et al.*, Phys. Rev. Lett. **86** 3500 (2001), see esp. [12]
 - [8] U. Heinz, nucl-th/0407067
 - [9] H.R. Collard, L.R.B. Elton, R. Hofstadter, Landolt-Bornstein, Numerical Data and Functional Relationships in Science and Technology, New Series, Volume 2, Nuclear Radii, Springer-Verlag 1967.
 - [10] K. Reygers, “Glauber Monte-Carlo Calculations for Au+Au Collisions at $\sqrt{S_{NN}} = 200$ GeV”, PHENIX Analysis Note 169,(2003).

Figures

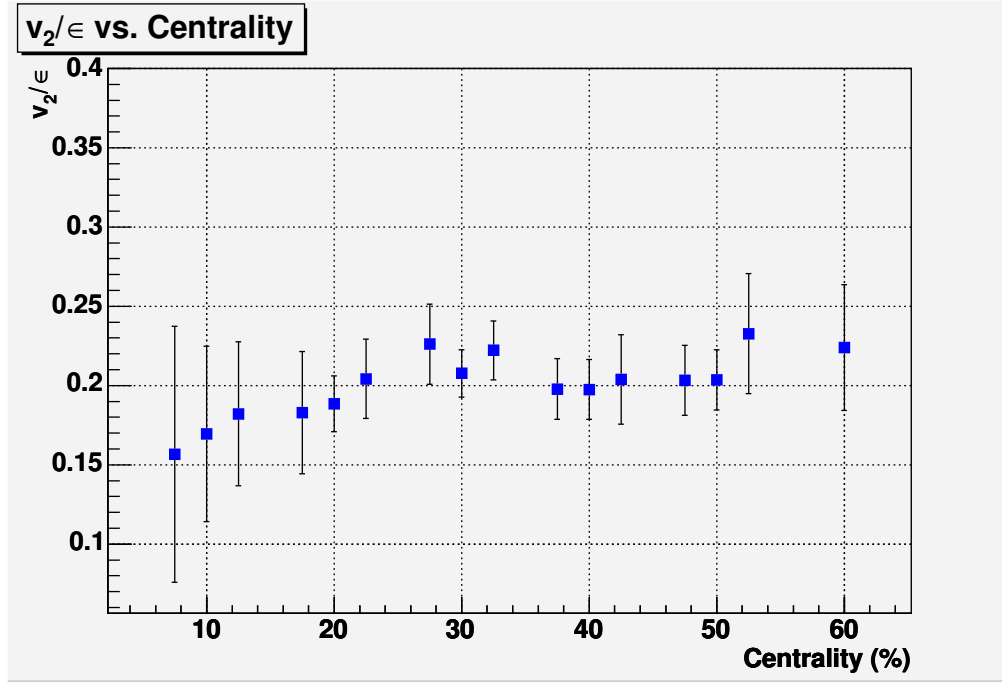
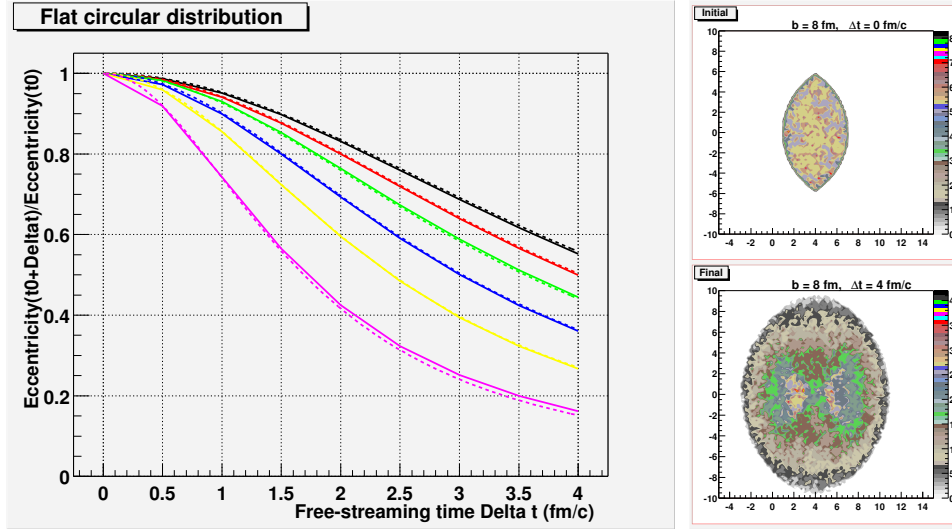


FIG. 1: PHENIX Data: v_2/ϵ vs. centrality for $Au+Au$ at $\sqrt{130}$ GeV for a p_T range of 0.4 - 0.6 GeV/c [6]. Note that the ratio remains within 20% of 0.2 for the entire centrality range shown. This suggests that the time evolution v_2 should be very similar to that of ϵ .



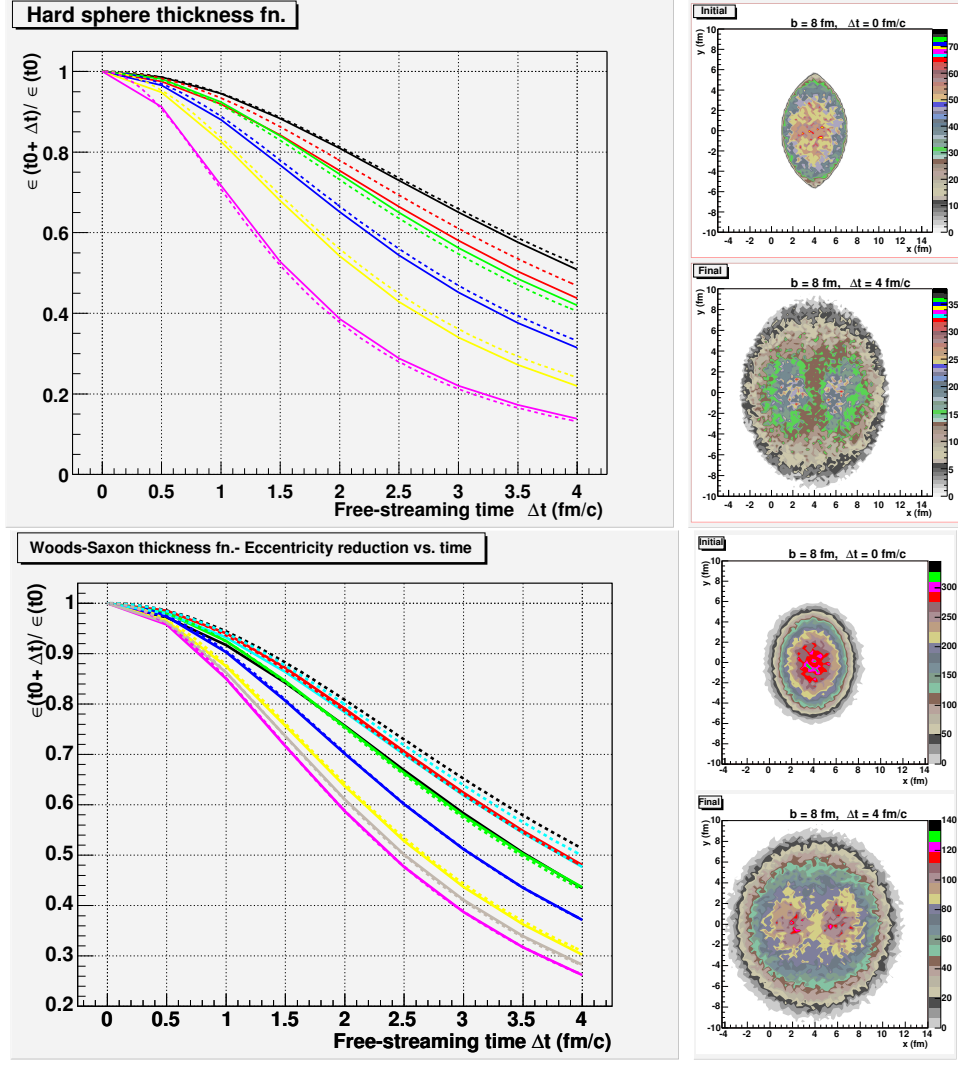


FIG. 2: Left Column: Eccentricity vs. time for the three particle distributions tested. Solid lines are from Monte Carlo simulations, dashed lines are plots of eq. (9). Right Column: Monte Carlo image of elliptical overlap region at time of impact (top) and after 4 fm/c of free-streaming. The plot colors correspond to impact parameters (in fm) as follows: black-2, red-4, green-6, blue-8, yellow-10, magenta-12.

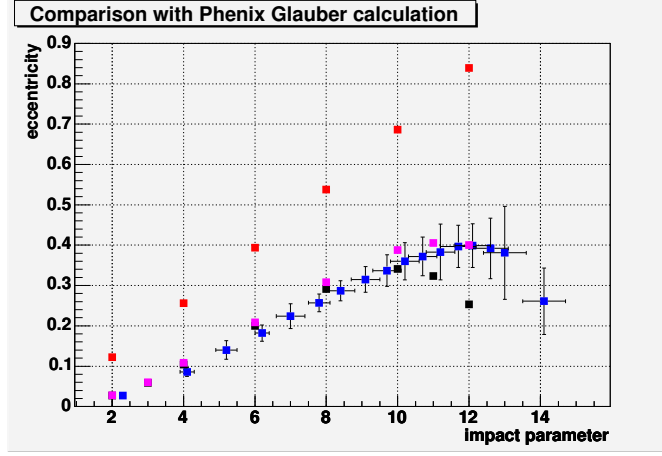


FIG. 3: Comparison of $\epsilon(t_0)$ values calculated in this analysis and those done by K. Reygers [10]. The blue points are from the Glauber model. The red points are for the hard-sphere approximation, the black for a full Woods-Saxon distribution, and the magenta points are for a Woods-Saxon profile which is truncated at $r_c = 10.3$ fm. The initial eccentricity is most sensitive to the value of r_c in more peripheral collisions.

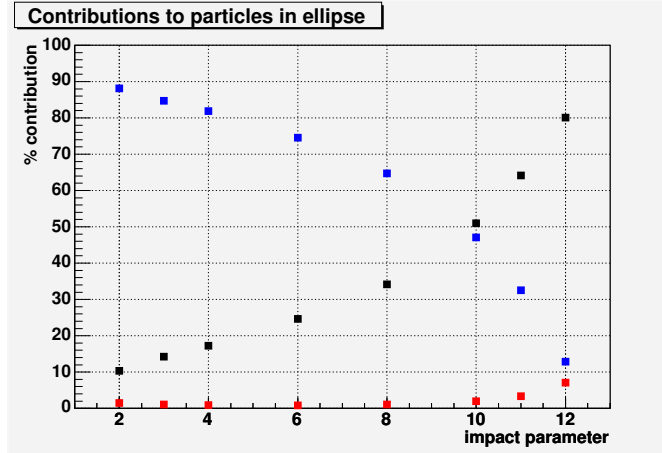


FIG. 4: Fractional contributions $r_{<} + r_{<}$ (blue), $r_{<} + r_{>}$ (black), and $r_{>} + r_{>}$ collision participants (red) to the initial eccentricity values. The $r_{<} + r_{>}$ contributions dominate the distribution at larger impact parameters but are significant even in the most central events.